A combined damage index for seismic assessment of non-ductile reinforced concrete structures
Mergos PE and Kappos AJ, Civil-Comp Proceedings, 2015

Abstract

Existing seismic damage indices have been formulated and verified almost exclusively on the basis of flexural damage mechanisms. In this paper, a local damage index proposed previously by the authors for assessing existing reinforced concrete (RC) structures is described. According to its formulation, deterioration caused by all deformation mechanisms (flexure, shear, anchorage slip) is treated separately for each mechanism. Moreover, the additive character of damage arising from the three response mechanisms, as well as the increase in degradation rate caused by their interaction, are fully taken into consideration. The proposed local damage index is first calibrated against experimental recordings and then is applied to predict seismic damage response of one RC column and one frame test specimen with substandard detailing. It is concluded that in all cases and independently from the prevailing mode of failure, the new local damage index predicts well the damage pattern of the analysed specimens.

Keywords: Reinforced concrete, damage index, substandard detailing, flexure, shear, bond-slip

.

1 Introduction

In Greece as well as in other countries often struck by devastating earthquakes, a large fraction of the existing RC building stock has not been designed to conform to modern seismic codes. These structures have not been detailed in a ductile manner and according to capacity design principles. Therefore, it is likely, that in case of a major seismic event, their structural elements will suffer from brittle types of failure, which may lead to irreparable damage or collapse of the entire structure.

In order to properly quantify structural damage reliable damage indices are required. A large number of seismic damage indices have been proposed in the

literature (Kappos [1], Cosenza and Manfredi [2]). The level of sophistication of the existing damage indicators varies from the simple and traditional displacement ductility to cumulative damage models which attempt to take into account damage caused by repeated cycling.

A major drawback of existing indices is that they have been formulated and verified almost exclusively on the basis of flexural damage mechanisms, possibly combining shear and bond-slip related mechanisms to the above, within the same constitutive law, e.g. moment-rotation. Following this approach, the contribution of each deformation mechanism to the total damage of a critical area of a member will be proportional to the participation of the rotation caused by this mechanism to the total rotation of this area. This may underestimate significantly damage arising from relatively stiff deformation mechanisms (e.g. shear), which contribute imperceptibly to the total rotation of the member.

The authors (Mergos and Kappos [3]) have proposed a new local damage index for existing reinforced concrete (RC) structures, wherein deterioration caused by all deformation mechanisms (flexure, shear, anchorage slip) is treated separately for each mechanism. Moreover, the additive character of damage arising from the three response mechanisms, as well as the increase in degradation rate caused by their interaction, are taken into consideration.

The proposed damage index is calibrated against experimental data involving damage evolution in 12 RC column specimens. To this cause, a new damage scale with three distinct damage levels for each deformation mechanism is introduced. Based on this damage scale and the experimental observations, the parameters of the proposed index are calibrated. Sufficient correlation is achieved with the experimental evidence. However, the need of further calibrating the damage index with experimental data is emphasized.

Furthermore, the local damage index is applied in conjunction with a finite element model developed by the authors (Mergos and Kappos [4]) to predict the damage state of several test specimens, including both individual RC columns and an entire frame with substandard detailing. It is concluded that in all cases and irrespective of the prevailing mode of failure, the new local damage index describes well the damage state of the analysed specimens up to the onset of failure.

2 Finite element modelling of RC members

The finite element model (Mergos and Kappos [4]) used herein for seismic damage analysis of existing RC structures is a beam-column element based on the flexibility approach (force-based element) and belongs to the class of phenomenological models.

The finite element model (Mergos and Kappos [4]) used herein for seismic damage analysis of existing RC structures is a beam-column element based on the flexibility approach (force-based element) and belongs to the class of phenomenological models.

It consists of three sub-elements representing flexural, shear, and anchorage slip response. The total flexibility of the finite element is calculated as the sum of the

flexibilities of its sub-elements and can be inverted to produce the element stiffness matrix.

The flexural sub-element is used for modelling flexural behaviour of an RC member before and after yielding of the longitudinal reinforcement. It consists of a set of rules governing the hysteretic moment-curvature (M-φ) response of the member end sections and a spread inelasticity model describing flexural stiffness distribution along the entire member (Mergos and Kappos [4]).

The M-φ hysteretic model is composed by the skeleton curve and a set of rules determining response during loading, unloading, and reloading. The M-φ envelope curve is derived by section analysis and appropriate bilinearization with corner points corresponding, as a rule, to yielding and failure.

Curvature capacity φ_u is considered as the minimum value from those corresponding to hoop fracture due to strain arising from the expansion of the concrete core, buckling of the longitudinal reinforcement, strength degradation exceeding 20% of the maximum moment capacity and fracture of the tension reinforcement in the tension zone.

Unloading is characterized by mild stiffness degradation; this is achieved by setting the unloading parameter of the Sivaselvan and Reinhorn [5] hysteretic model equal to 15. Reloading aims at the point with previous maximum excursion in the opposite direction.

The shear sub-element models the hysteretic shear behaviour of the RC member prior and subsequent to shear cracking, flexural yielding and yielding of the transverse reinforcement. This sub-element has been designed in a similar way to the flexural element described above. It consists of a hysteretic model determining V-γ (shear force vs. shear deformation) behaviour of the member ends and/or intermediate regions and a shear spread-plasticity model determining distribution of shear stiffness along the RC member (Mergos and Kappos [4]).

Shear hysteresis is modelled using the V-γ skeleton curve described subsequently and the empirical hysteretic model by Ozcebe & Saatcioglu [6] and appropriate modifications introduced by the writers of this study (Mergos and Kappos [7]).

The primary (skeleton) curve is first determined without considering shear-flexure interaction. This initial envelope curve (Figure 1a) is valid for modelling shear behaviour outside the plastic hinge region for members that have yielded in flexure, or the response of the entire element for members, where the longitudinal reinforcement remains in the elastic range.

The V-γ initial primary curve consists of four branches, but only three different slopes, as explained later on. The first branch connects the origin and the shear cracking point, which is defined as the point where the nominal principal tensile stress exceeds the tensile strength of concrete. The second and third branches of the primary curve have the same slope and connect the shear cracking point (γ_{cr}, V_{cr}) to the point corresponding to the onset of yielding of transverse reinforcement, or else the point of attainment of maximum shear strength (γ_{st},V_{uo}). The second and third branches are separated at the point corresponding to flexural yielding (γ_y,V_y). The fourth branch is almost horizontal (stiffness close to zero) and extends up to the point of onset of shear failure (γ_u,V_{uo}).

Shear strain γ_{st} is calculated by the respective shear strain γ_{truss} calculated by the truss analogy approach (Park and Paulay [8]), for an angle between the element axis and the concrete compression struts $\theta=45^o$, and two modification factors proposed by the authors (Mergos and Kappos [4]) to account for member aspect ratio and normalized axial load. Shear strain γ_u is calculated from an empirical formula proposed again by the authors (Mergos and Kappos [4]) on the basis of experimental data from 25 RC specimens failing in shear.

It is well documented that shear strength of concrete resisting mechanisms V_c degrades due to disintegration of the plastic hinge zones caused by inelastic flexural deformations. Additionally, it has been shown experimentally that shear strains increase rapidly in plastic hinge regions following flexural yielding. This combined phenomenon is characterized in the following as shear-flexure interaction effect.
The authors (Mergos and Kappos [4]) have developed a methodology for defining the V-γ envelope curve incorporating interaction with flexure. According to this procedure, the shear strain γ after flexural yielding and prior to stirrup yielding is given by Equation 1, where GA_1 is the cracked shear stiffness of the initial envelope given by Equation 2, V_{st} is the shear force carried by the transverse reinforcement, V is the applied shear force and $\deg V_c$ is the total drop in the concrete mechanism shear strength capacity V_c for the curvature ductility demand μ_φ corresponding to V. $\deg V_c$ may be determined by a shear strength model accounting for degradation of V_c with μ_φ, such as the one described in Priestley *et al*. [9]. It is noted that at stirrup yielding, it becomes $V_{st}=V_w$, where V_w is the shear strength capacity of the transverse reinforcement.

$$\gamma = \gamma_{cr} + \frac{V_{st}}{GA_1} = \gamma_{cr} + \frac{V - V_{cr} + \deg V_c}{GA_1} \tag{1}$$

$$GA_1 = \frac{V_{uo} - V_{cr}}{\gamma_{st} - \gamma_{cr}} \tag{2}$$

The bond-slip sub-element accounts for the fixed-end rotations (θ_{sl}) which arise at the interfaces of adjacent RC members due to bond deterioration and slippage of the reinforcement in the joint regions and the lap splices. The proposed model consists of two concentrated rotational springs located at the member ends (Mergos and Kappos [4]). The two (uncoupled) springs are connected by an infinitely rigid bar.

The M-θ_{sl} skeleton curve is derived on the basis of a simplified procedure Mergos and Kappos [4] assuming uniform bond stress along different segments of the anchored rebar. These segments are the elastic region, the strain-hardening region and the cone penetration zone. Following this assumption, stress and strain distribution is determined and reinforcement slippage δ_{sl} is calculated for each step of end section M-φ analysis by integrating rebar strains along the anchorage length. Finally, by dividing δ_{sl} by the distance of the anchored bar to the neutral axis depth, the respective fixed-end rotation θ_{sl} is defined.

The envelope M-θ_{sl} curve defined by the various points of the afore-described methodology is then idealized by a bilinear relationship with the corner points

corresponding to yielding and failure. After defining M-θ_{sl} bilinear envelope, bond-slip hysteresis is modelled following the suggestions of Saatcioglu and Alsiwat [10].

In the presence of lap splices, additional fixed-end rotations θ_{lap} arising from slippage of the reinforcement in the splice regions should be added to θ_{sl}. A very common deficiency in under-designed RC structures is the existence of very short lap splices in the locations of the potential plastic hinges. These splices were designed solely for compression. Hence, under tension loading imposed by earthquakes, these splices frequently fail prior to yielding of the longitudinal reinforcement.

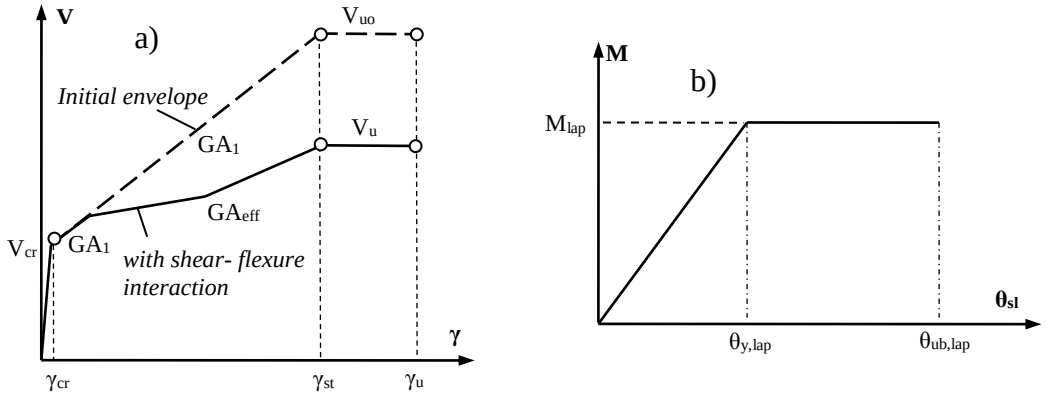

Figure 1: a) Shear (V – γ) primary curve before and after modelling shear-flexure interaction; b) Bilinear approximation of the M-θ_{sl} response of RC member ends with poor lap splices (Mergos and Kappos [3]).

Melek *et al*. [11] investigated the experimental response of such column lap splices. They concluded that the average bond strength of these splices is approximately $u_{lap}=0.95\sqrt{f_c}$. This value is also adopted herein for determining ultimate moment capacity M_{lap} of inadequate lap splices.

Fixed-end rotation $\theta_{y,lap}$ corresponding to attainment of M_{lap} is determined by adding the respective fixed-end rotations developed along the anchorage and lap splice length. Fixed-end rotations arising from poor lap splices are determined by assuming uniform bond strength u_{lap} along the splice length. The fixed-end rotation $\theta_{ub,lap}$ corresponding to 20% drop in the lap splice moment capacity is determined by Equation 3 (Mergos and Kappos [3]).

$$\theta_{ub,lap} = \theta_{y,lap} + 0.005 \tag{3}$$

3 Local damage index

By definition, a seismic damage index is a quantity with zero value when no damage occurs and equal to 1 (100%), when failure occurs. However, a non-ductile RC

member may fail either in flexure or in shear or due to loss of bond (in an anchorage or lap-splice zone). Hence, an appropriate local seismic damage index, D_{tot}, for such a member should assume unity value when the respective end of the member reaches its flexural *or* shear *or* bond-slip deformation capacity.

A general mathematical relationship proposed by the authors (Mergos and Kappos [3]) that satisfies the aforementioned limitations is

$$D_{tot} = 1-\left(1-D_{fl}\right)\cdot\left(1-D_{sh}\right)\cdot\left(1-D_{sl}\right) \tag{4}$$

where D_{tot} is the total local damage index ($0\leq D_{tot}\leq 1$) representing total damage at the member end; D_{fl} is the flexural damage index ($0\leq D_{fl}\leq 1$), representing flexural damage at the member end; D_{sh} is the shear damage index ($0\leq D_{sh}\leq 1$) representing shear damage at the member end; D_{sl} is the bond slip damage index ($0\leq D_{sl}\leq 1$) representing bond slip damage at the member end.

It is evident that when one of the damage indices D_i becomes equal to one (flexural, shear of bond failure) then D_{tot} becomes equal to one as well, irrespective of the value of the other indices. For all other intermediate values of D_i (i=1,2,3), D_{tot} becomes always equal or greater than $D_{max,}$ where D_{max} is the maximum value of the individual indices D_i. In this way, the combined deterioration effect caused by the three individual damage mechanisms (flexure, shear, bond) is explicitly taken into account.

It is evident that for the calculation of total damage index D_{tot} determination of individual damage indices D_{fl}, D_{sh} and D_{sl} is first required. In general, damage in RC elements is related to deformations. Therefore, any damage variable should preferably refer to a certain deformation quantity (Kappos [1]).

By definition, the flexural damage index D_{fl} should refer to a local, purely flexural, deformation variable. The best choice for this case is the curvature φ developed at the respective end of the member. In a similar fashion, shear damage index D_{sh} should refer to the shear distortion developed at the respective end region of the RC member. Lastly, bond-slip damage index D_{sl} has to be correlated with fixed-end rotation θ_{sl}.

Taking the above into consideration, Equation 5 can be used for D_{tot} determination, where $\varphi_{max,}$ γ_{max} and $\theta_{sl,max}$ are maximum developed curvature, shear distortion and fixed-end rotation respectively at the member end.

$$D_{tot} = 1-\left(1-\left(\frac{\varphi_{\max}}{\varphi_u}\right)^{\lambda_{fl}}\right)\cdot\left(1-\left(\frac{\gamma_{\max}}{\gamma_u}\right)^{\lambda_{sh}}\right)\cdot\left(1-\left(\frac{\theta_{sl,\max}}{\theta_{ub,sl}}\right)^{\lambda_{sl}}\right) \tag{5}$$

In these equations, λ_{fl}, λ_{sh} and λ_{sl} are exponents determining the rate at which flexural, shear, or bond, damage increases with the normalized ratios φ_{max}/φ_u, γ_{max}/γ_u and $\theta_{sl,max}/\theta_{ub,sl}$ respectively. It is evident that the values of λ_{fl}, λ_{sh}, λ_{sl} may have a vital influence on the final outcome of D_{tot}. Clearly, these exponents should be calibrated on the basis of experimental evidence.

The first step to calibrate the damage index coefficients is to define an appropriate damage scale for each type of structural damage. The damage scales adopted by the authors (Mergos and Kappos [3]) for each deformation mechanism are presented in Table 1.

Damage Level	Flexural damage	Shear damage	Bond damage	Damage Index
(A) Minor damage	Flexural cracks (<2 mm). Limited yielding. No spalling.	Hairline-minor shear cracks (<0.5 mm)	Fixed-end cracks (<2 mm). Hairline – visible bond cracks in parts of the lap splices	0.00-0.20
(B) Moderate damage	Spalling of concrete cover	Moderate shear cracking (>0.5 mm)	Fixed-end cracks (>2 mm). Moderate bond cracking in parts of the lap splices	0.20-0.50
(C) Severe damage	Buckling of compressive reinforcement, core concrete disintegration, fracture of tensile reinforcement, yielding or fracture of transverse reinforcement due to core expansion.	Severe shear cracking (>1 mm), stirrup yielding or fracture.	Major fixed-end cracks indicating reinforcement pullout. Severe bond cracking along the full length of the lap splices. Spalling of cover surrounding lap-spliced bars	0.50-1.00

Table 1: Adopted scale for flexural, shear and bond damage mechanisms of RC member critical regions (Mergos and Kappos [3]).

The second step of the damage index calibration process is the correlation of the damage index values to the damage scales described above. The damage index values adopted by the authors (Mergos and Kappos [3]) to represent the different levels of the damage scale are also presented in Table 1.

As a final step, the calibration of λ_{fl}, λ_{sh}, λ_{sl} coefficients has to take place. The authors (Mergos and Kappos 2013) calibrated these coefficients against 12 RC column specimens that experienced different types of failure. For all of these specimens a detailed description of their damage progression is available, something not common in the pertinent literature. Four of them developed flexural failures, four failed in shear mode and four of them experienced bond-slip type of failure. The latter failed due to bond deterioration of their deficient lap splices (Melek *et al*. [11]).

For each specimen, displacement-controlled pushover analysis was conducted up to the level of experimental lateral displacement ductility $\mu_{\Delta u}$ corresponding to the onset of significant lateral strength degradation (D_{tot}=1.0), by applying the finite element model described in the previous chapter of this paper. The pushover analysis calculated normalized deformation ratios φ/φ_u, γ/γ_u and $\theta_{sl}/\theta_{ub,sl}$ for different levels of the imposed ductility demands μ_Δ.

Moreover, following the experimental observations regarding all damage modes (flexure, shear, bond) for all RC specimens and imposed displacement ductilities (drifts), the experimental individual damage indices D_{fl}^{exp}, D_{sh}^{exp}, D_{sl}^{exp} are estimated in accordance with the damage scales described in Table 1. It is important to mention here that the experimental damage index values have been derived from

the final loading cycle at each imposed ductility (drift) level. In this way, additional degradation due to cyclic loading effects is taken indirectly into account in the analytical procedure.
Having established the experimental D_{fl}^{exp}, D_{sh}^{exp} and D_{sl}^{exp} values for the different calculated normalized ratios φ/φ_u, γ/γ_u and $\theta_{sl}/\theta_{ub,sl}$, nonlinear regression analyses are conducted to evaluate the values of λ_{fl}, λ_{sh} and λ_{sl}, which provide maximum correlation between the predicted by D_{fl}^{pred}, D_{sh}^{pred}, D_{sl}^{pred} damage index values and their experimental counterparts. Based on these analyses, values of exponents λ_{fl}, λ_{sh} and λ_{sl} are found to be equal to 1.35, 0.95 and 0.80 respectively.

In line with the aforementioned observations, Equation 6 was proposed to determine total damage index D_{tot} of the critical end region of an RC member as a function of its individual normalized deformation ratios.

$$D_{tot} = 1 - \left(1 - \left(\frac{\varphi_{\max}}{\varphi_u}\right)^{1.35}\right) \cdot \left(1 - \left(\frac{\gamma_{\max}}{\gamma_u}\right)^{0.80}\right) \cdot \left(1 - \left(\frac{\theta_{sl,\max}}{\theta_{ub,sl}}\right)^{0.95}\right) \quad (6)$$

4 Validation of the proposed damage index

The member-type finite element model developed by the authors and the local damage index described herein have been implemented in the computer program IDARC2D for the nonlinear dynamic analysis of 2D RC structures. To validate the proposed damage model, this program was used to simulate the hysteretic response of several experimental RC columns and frames tested under cyclic or loading, exhibiting different types of failure. In the following, the analytical predictions for a single column specimen and a frame structure are presented.

4.1 Lehman and Moehle [12] column specimen 415

Lehman and Moehle (1998) tested five circular RC bridge columns, typical of modern construction, under uniaxial displacement-controlled lateral load reversals in single bending. Herein, the specimen designated as 415 (Figure 2a) is studied. This specimen was dominated by flexure, exhibiting stable hysteretic behaviour until failure occurred at a ductility $\mu_{\Delta u} \approx 7$. The specimen was subjected to a constant axial load of 654 kN. Concrete strength was 31 MPa and yield strengths of longitudinal and transverse reinforcement were 510 MPa and 607 MPa, respectively.

Figure 2b shows the experimental and analytical lateral load vs. total displacement relationship of the specimen. It is seen that the proposed analytical model predicts well the experimental behaviour up to maximum response.

Figure 2c shows the development of the individual damage indices D_{fl}, D_{sh} and D_{sl} as a function of the imposed lateral displacement ductility demand, as predicted by the analytical model of this study and as described in the experimental report. In general, very good agreement is observed over the entire range of response.

Finally, Figure 2d illustrates the evolution of the damage profile of the examined RC specimen. It can be seen that shear damage remains minor, while bond damage (base cracking) becomes moderate at the end of the analysis. However, flexural damage governs the response of this member and at the end of the analysis D_{fl} becomes equal to unity, indicating a flexural type of failure.

Due to its formulation, the total damage index remains greater than each individual damage index during the entire loading sequence. In this way, combined damage by the individual deformation mechanisms is taken into consideration. At the final step of the analysis, D_{tot} is restrained by D_{fl} and becomes equal to unity as well, revealing the failure damage state of the specimen under examination.

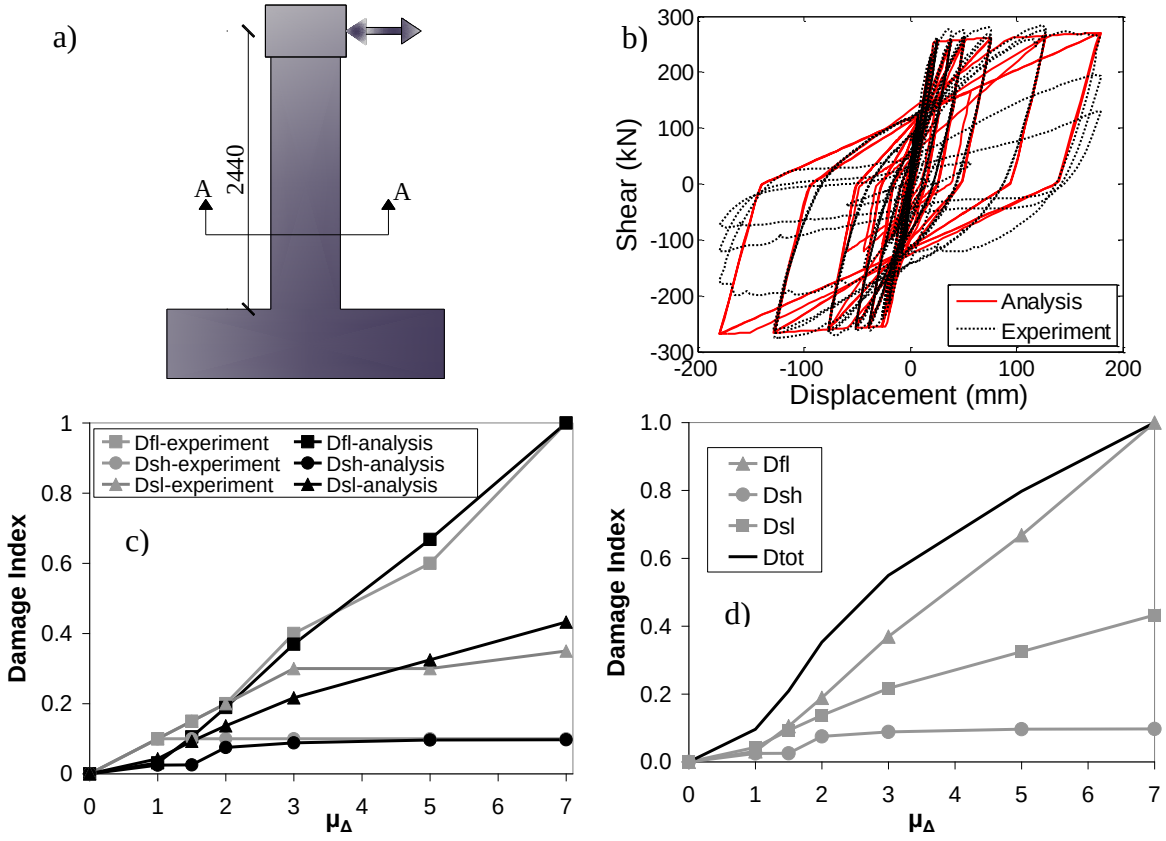

Figure 2: Lehman & Moehle (1998) specimen 415: (a) Specimen configuration; (b) Lateral load vs. lateral displacement; (c) Variation of the predicted and experimental individual indices with μ_Δ; (d) Evolution of the analytical damage profile of the RC member (Mergos and Kappos [3]).

4.2 Duong *et al.* [13] frame specimen

This single-bay, two-storey frame (Figure 3a) was tested by Duong *et al.* (2007) at University of Toronto. The frame was subjected to a single loading cycle. During the experiment, a lateral load was applied to the second storey beam in a

displacement-control mode, while two constant axial loads were applied throughout the testing procedure to simulate the axial load effects of upper stories (Figure 3a). During loading sequence, the two beams of the frame experienced significant shear damage (close to shear failure) following flexural yielding at their ends. The finite element model applied in this study to predict frame specimen response is also shown in Figure 3a.

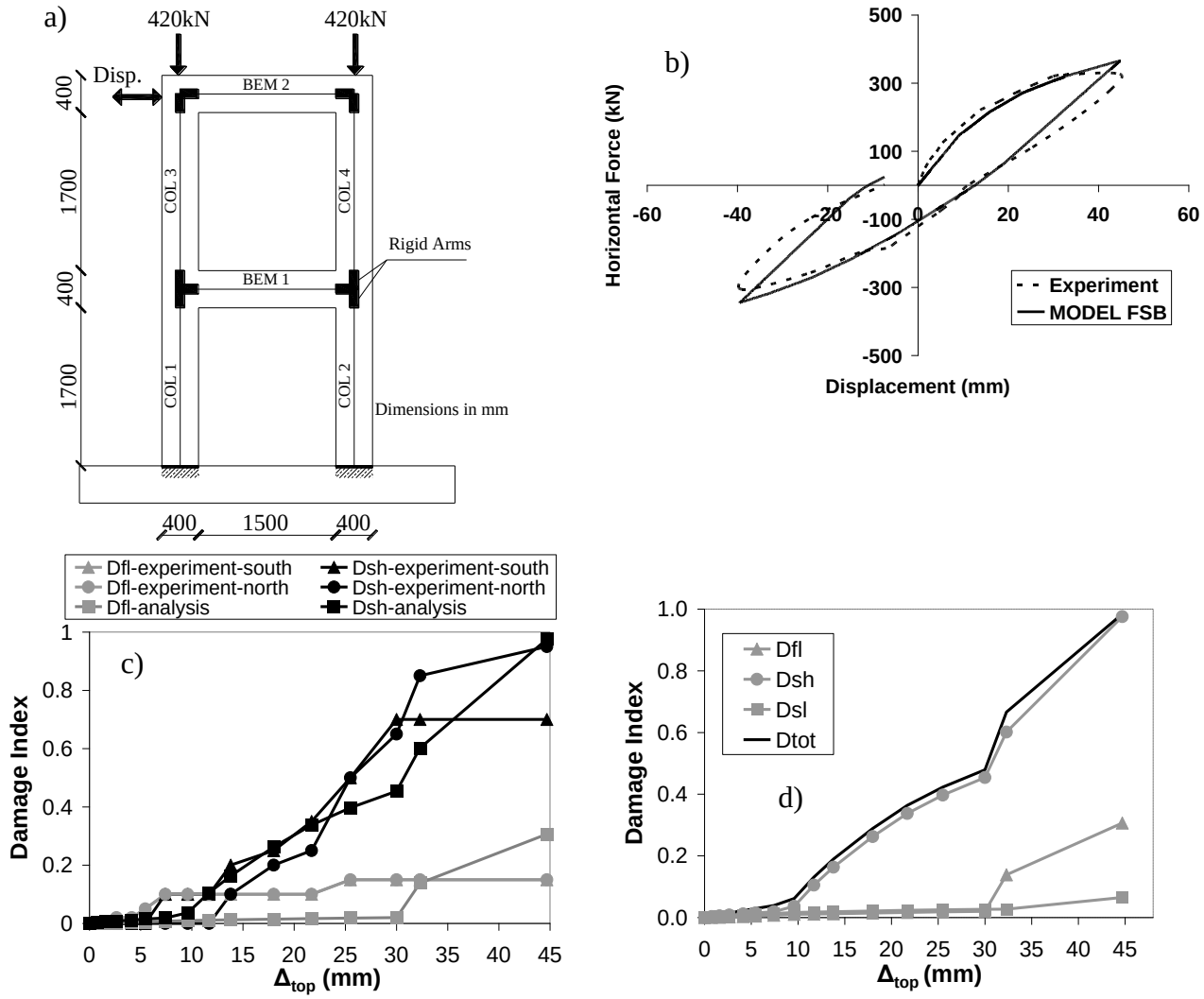

Figure 3: Duong *et al*. (2007) frame specimen: (a) Specimen configuration; (b) Base shear vs. top displacement frame response; (c) Predicted and experimental individual damage indices of the 1st storey beam; (d) Analytical damage indices progression for the 1st storey beam (Mergos and Kappos [4]).

As illustrated in Figure 3b, the analytical model follows sufficiently close the experimental behaviour over the entire range of response. In addition, the analytical model predicts that both beams develop shear failure after yielding in flexure, as

observed in the experimental procedure. Furthermore, it is worth noting that damage to columns of this RC frame was reported to be minor, in close agreement with the analytical prediction.

Figures 3c and 3d present experimental and analytical damage indices progression with the top frame displacement in the positive direction of loading for the first storey RC beam. At the end of loading in this direction, severe shear cracking was detected in this element with a 9 mm wide shear crack indicating imminent shear failure.

Figure 3c presents the comparison of the predicted and the experimental individual flexural and shear damage indices for the 1st storey beam. Despite the symmetrical configuration of the RC frame, shear damage was found in the test to differ between the north and south beam ends. Hence, experimental damage propagation for both beam ends is presented.

The analytical model predicts the same structural damage for both beam ends and the predicted damage indices reasonably match their experimental counterparts. Flexural damage is slightly underestimated in the first stages of loading, but is predicted well at the end of the analysis. Shear damage is predicted to be major-to-severe for this beam member. More particularly, D_{sh} is predicted to be very close to unity (0.97) indicating shear failure in accordance with the experimental observations.

Figure 3d illustrates the development of the predicted damage profiles with the imposed lateral top displacement again for the 1st storey beam. It can be seen that shear damage almost completely governs the response and D_{tot} is only marginally greater than D_{sh} for both members. At the end of the analysis, D_{tot} becomes 0.98 for this beam member, indicating imminent shear failure.

5 Conclusions

A new combined local damage index for existing RC members has been proposed by the authors (Mergos and Kappos [3]), which treats degradation caused by all deformation mechanisms (flexure, shear, bond-slip) in an explicit and discrete manner. The index is capable of capturing the additive character of deterioration coming from the three inelastic response mechanisms, as well as the increase in damage caused by their interaction.

The proposed damage index has been calibrated against experimental data involving damage evolution in 12 RC column specimens. To this cause, a new damage scale with three distinct damage levels for each deformation mechanism is introduced. Based on this damage scale and the experimental observations, the parameters of the proposed index are calibrated. Sufficient correlation is achieved with the experimental evidence. However, the need of further calibrating the damage index with experimental data is emphasized.

Next, the local damage index was applied in conjunction with a finite element model developed by the authors (Mergos and Kappos [4]) to predict the damage state of several test specimens, including both single RC columns and an entire frame with substandard detailing. It is concluded that in all cases and irrespective of

the prevailing mode of failure, the new local damage index describes well the damage state of the analysed specimens up to the onset of failure. Further research is required towards modelling structural response and quantifying structural damage in the post peak range of response.

References

[1] A.J. Kappos, "Seismic damage indices for RC buildings: evaluation of concepts and procedures", Progress in Structural Engineering and Materials, 1 (1), 78-87, 1997.

[2] E. Cosenza, G. Manfredi, "Damage indices and damage measures", Progress in Structural Engineering and Materials, 2 (1), 50-59, 2000.

[3] P.E. Mergos, A.J. Kappos, "A combined local damage index for seismic assessment of existing R/C structures", Earthquake Engineering and Structural Dynamics, 42(6), 833-852, 2013.

[4] P.E. Mergos, A.J. Kappos, "A gradual spread inelasticity model for R/C beam-columns, accounting for flexure, shear and anchorage slip", Engineering Structures, **44,** 94-106, 2012.

[5] M.V. Sivaselvan, A.M. Reinhorn, "Hysteretic models for deteriorating inelastic structures" Journal of Engineering Mechanics, 126(6), 633-640, 2000.

[6] G. Ozcebe, M. Saatcioglu, "Hysteretic shear model for reinforced concrete members", Journal of Structural Engineering, 115 (1), 132-148, 1989.

[7] Mergos PE, Kappos AJ (2008). A distributed shear and flexural flexibility model with shear-flexure interaction for RC members subjected to seismic loading. *Earthquake Engineering and Structural Dynamics*; **37** (12): 1349-1370.

[8] R. Park, T. Paulay, "Reinforced concrete structures", Wiley: New York, 1975.

[9] M.J.N. Priestley, R. Verma, Y. Xiao, "Seismic shear strength of reinforced concrete columns", Journal of Structural Engineering (ASCE), 120(8), 2310-2329, 1994.

[10] J.M. Alsiwat, M. Saatcioglu, "Reinforcement anchorage slip under monotonic loading", Journal of Structural Engineering, 118(9), 2421-2438, 1992.

[11] M. Melek, J.W. Wallace, J.P. Conte, "Experimental assessment of columns with short lap splices subjected to cyclic loads", PEER Report 2003/04, Univ. California, Berkeley, 2004.

[12] D. Lehman, J.P. Moehle, "Seismic performance of well confined concrete bridge columns", PEER Report 1998/01, Univ. of California, Berkeley, 1998.

[13] K.V. Duong, F.J. Sheikh, F. Vecchio, "Seismic behaviour of shear critical reinforced concrete frame: Experimental Investigation", ACI Structural Journal, 104(3), 304-313, 2007.